

Presented at DIS2022: XXIX International Workshop on Deep-Inelastic Scattering and Related Subjects
 Santiago de Compostela, Spain, May 2-6 2022

Inclusive J/ψ and Υ emissions from single-parton fragmentation in hybrid high-energy and collinear factorization

Francesco Giovanni Celiberto ^{a,1,2,3} , Michael Fucilla ^{b,4,5,6} 

¹European Centre for Theoretical Studies in Nuclear Physics and Related Areas (ECT*), I-38123 Villazzano, Trento, Italy

²Fondazione Bruno Kessler (FBK), I-38123 Povo, Trento, Italy

³INFN-TIFPA Trento Institute of Fundamental Physics and Applications, I-38123 Povo, Trento, Italy

⁴Dipartimento di Fisica, Università della Calabria, I-87036 Arcavacata di Rende, Cosenza, Italy

⁵Istituto Nazionale di Fisica Nucleare, Gruppo collegato di Cosenza, I-87036 Arcavacata di Rende, Cosenza, Italy

⁶Université Paris-Saclay, CNRS, IJCLab, 91405 Orsay, France

August 16, 2022

Abstract

We present a novel study on the inclusive production of a heavy quarkonium (J/ψ or Υ), in association with a light-flavored jet, as a test field of the high-energy QCD dynamics. The large transverse momenta at which the two final-state objects are detected permits us to perform an analysis in the spirit of the variable-flavor number scheme (VFNS), in which the cross section for the hadroproduction of a light parton is convoluted with a perturbative fragmentation function that describes the transition from a light quark to a heavy hadron. The quarkonium collinear fragmentation function is built as a product between a short-distance coefficient function, which encodes the resummation of DGLAP type logarithms, and a non-perturbative long-distance matrix element (LDME), calculated in the non-relativistic QCD (NRQCD) framework. Our theoretical setup is the hybrid high-energy and collinear factorization, where the standard collinear approach is supplemented by the resummation of leading and next-to-leading energy-type logarithms *à la* BFKL. We propose this reaction as a

suitable channel to probe the production mechanisms of quarkonia at high energies and large transverse momenta and to possibly unveil the transition region from the heavy-quark pair production mechanism to the single-parton fragmentation one.

KEYWORDS:

QCD phenomenology
 high-energy resummation
 quarkonium production
 NRQCD fragmentation

1 Introduction

In this work we focus on the high-energy inclusive hadroproduction of a heavy vector mesons. The energies reachable at the Large Hadron Collider (LHC) and at new-generation hadron accelerators [1–22] permits us to access kinematic regions where $\sqrt{s} \gg m_Q$, with m_Q the vector mass. In this case, the so-called *Regge-Gribov*

^ae-mail: fceliberto@ectstar.eu

^be-mail: michael.fucilla@unical.it (corresponding author)

or *semi-hard* regime [23, 24] of QCD, characterized by $\sqrt{s} \gg \{Q\} \gg \Lambda_{\text{QCD}}$, is reached.¹ As it is well known, in this regime, large energy-type logarithms appear to all orders in perturbation theory with a power increasing with the α_s order, thus spoiling the convergence of the perturbative series obtained within the standard fixed-order approach. A resummation to all orders, that takes into account the effect of these logarithms, it is strictly necessary to build concrete predictions in this regime. The most powerful formalism for the description of the semi-hard QCD sector is the Balitsky–Fadin–Kuraev–Lipatov (BFKL) approach [25–28], which is valid in the leading approximation (LLA), *i.e.* $\alpha_s^n \ln(s/Q^2)^n$ terms are resummed, and within the next-to-leading approximation (NLA), *i.e.* also $\alpha_s^{n+1} \ln(s/Q^2)^n$ terms are also included.

BFKL-resummed cross sections are elegantly portrayed by a high-energy convolution between a universal, energy-dependent Green's function, and two impact factors depicting the transition from each incoming particle to the outgoing object(s) produced in its fragmentation region. The BFKL Green's function satisfies an integral evolution equation, whose kernel is known up to NLO for any fixed, not growing with s , momentum transfer t and for any possible two-gluon color state in the t -channel [29–35]. Impact factors instead depend on processes, so they represent the most challenging part of the calculation. Few of them are known within NLO accuracy.

Combining pairwise the available NLO impact factors, a number of semi-hard (inclusive) reactions can be described within the BFKL approach in the NLA and predictions can be formulated, mainly in the form of azimuthal correlations or transverse momentum distributions, most of them accessible to current experiments at the LHC. These reactions include: the inclusive detection of two light jets featuring large transverse momenta and well separated in rapidity (Mueller–Navelet channel [36]), for which several phenomenological studies have appeared so far [37–52]), the inclusive emission of a light di-hadron system [53–57], multi-jet tags [58–71],

¹Here s is the center-of-mass energy squared, $\{Q\}$ represents the (set of) perturbative scale(s) characterizing the process, and Λ_{QCD} stands for the QCD scale parameter.

hadron-jet [72–75], Higgs-jet [76–81], Drell–Yan-plus-jet [82], hadrons with heavy flavor [83–94], and heavy-light di-jet systems [95, 96].

It is well known that phenomenological studies of semi-hard processes feature instabilities of the BFKL series under higher-order corrections and scale variations, preventing us to carry out analyses around *natural* scales of the process, namely the ones dictated by kinematics. Some scale-optimization procedures, such as the Brodsky–Lepage–Mackenzie (BLM) procedure [97–100] one, can help to reduce these instabilities in reactions featuring the emissions of light jets and/or hadrons [40, 42, 53, 55]. Nevertheless, the optimal-scale values predicted by the procedure are much higher than the natural ones [101]. This leads to a lowering of cross sections of one or more orders of magnitude.

A first sign of stability was observed in partial NLA analyses, involving impact factors characterized by the presence of a particle having a large transverse mass, as Higgs bosons [76, 94] and heavy-quark jets [95]. Until now, however, the lack of Higgs and heavy quark NLO impact factors has prevented the confirmation of these stability in a full NLL analysis.²

Recently, it was pointed out that stabilization effects in full NLA observables emerge in a variable-flavor number-scheme (VFNS) [103, 104] treatment of charmed and bottomed hadrons' production [88, 89]. In particular, it has been found that peculiar pattern of VFNS fragmentation functions (FFs), depicting the production of heavy hadrons at large transverse momentum, acts as a fair stabilizer of the high-energy series.

In this article we investigate the high-energy behavior of the inclusive hadroproduction of a J/ψ or a Υ accompanied by a light-quark jet at the LHC. Both the meson and the jet feature large transverse momenta, and they are well separated in rapidity. The large required transverse momenta makes valid using the variable-flavor number-scheme (VFNS) approach. In this spirit, we will combine three main objects: 1) parton distribution functions (PDFs), 2) cross sections for the production of a light parton, 3) FFs describing the transition from

²The forward Higgs-boson impact factor has been recently calculated at NLO (see Refs. [81, 102] for novel calculations), but its numerical implementation is not yet available.

light quarks to heavy bound states (J/ψ or Υ). The latters represent new ingredients enriching our hybrid high-energy and collinear factorization already set as the reference formalism for the description of inclusive two-particle semi-hard emissions. Quarkonium FFs at the initial scale are constructed, within the framework of NRQCD, as a product between a short-distance coefficient function, depicting the transition from a heavy quark to the Fock state of the produced hadron, and the corresponding LDME. At this point, the DGLAP evolution comes into play. Indeed, when the transverse momenta of the parton produced in the initial hard scattering is sufficiently larger than the production threshold, the heavy quark can be dynamically generated through a cascade of collinear emissions. Therefore, what within the context of the VFNS we could define as perturbative FF is constructed in two steps: the first in which the transition from light to heavy parton takes place and one in which the heavy parton produces the quarkonium according to the dictates of NRQCD. We will employ a recent NLO determination for heavy-quark to J/ψ and Υ FFs [105].

As already mentioned, the fragmentation mechanism becomes increasingly competitive as well as the transverse momentum of the produced quarkonium grows. We remind, however, that since we are neglecting the heavy-quark mass at the level of the hard part, our formalism is not suited to properly describe the intermediate region, where $|\vec{p}_T| \sim m_Q$. Here, powers of the $\sqrt{m_Q^2 + |\vec{p}_T|^2}/|\vec{p}_T|$ ratio need to be taken into account. In this sense, our study is complementary to the one proposed in Ref. [83] (see also preliminary results in Refs. [106, 107]), where the inclusive semi-hard J/ψ -plus-jet production was investigated by making use of the short-distance ($Q\bar{Q}$) mechanism for the quarkonium production. In such a calculation all powers of the ratio $\sqrt{m_Q^2 + |\vec{p}_T|^2}/|\vec{p}_T|$ are present, but since the final state features no DGLAP evolution, collinear logarithms are not resummed.

2 Hybrid high-energy and collinear factorization

The process under investigation is

$$p(P_a) + p(P_b) \rightarrow \mathcal{Q}(p_Q, y_Q) + X + \text{jet}(p_J, y_J), \quad (1)$$

where $p(P_{a,b})$ indicate an initial proton with momentum $P_{a,b}$, $\mathcal{Q}(p_Q, y_Q)$ stands for J/ψ or Υ emitted with momentum p_Q and rapidity y_Q , p_J and y_J are the transverse momenta and rapidity of the produced light jet and X denotes the undetected remnant of the reaction. The diffractive semi-hard configuration in the final state is obtained by requiring a large rapidity separation $\Delta Y = y_Q - y_J$ and high observed transverse momenta, $|\vec{p}_{Q,J}|$. Moreover, a large transverse-momentum is required in order to ensure of a VFNS treatment of the quarkonium fragmentation.

We introduce the standard Sudakov decomposition for the four-momenta of final-state particles,

$$p_{Q,J} = x_{Q,J} P_{a,b} + \frac{\vec{p}_{Q,J}^2}{x_{Q,J}s} P_{b,a} + p_{Q,J\perp} \quad (2)$$

with $p_{Q,J\perp}^2 = -\vec{p}_{Q,J}^2$,

and where we choose P_a and P_b as light cone basis, *i.e.* $P_a^2 = P_b^2 = 0$ and $s = 2(P_a \cdot P_b)$. The longitudinal momentum fractions, $x_{Q,J}$, are related to the corresponding rapidities by the relation

$$y_{Q,J} = \pm \frac{1}{2} \ln \frac{x_{Q,J}s}{\vec{p}_{Q,J}^2}. \quad (3)$$

In collinear factorization, the LO cross section of our process (Eq. (1)) is given by the convolution of the partonic hard sub-process with the parent-proton PDFs and the quarkonium FFs

$$\begin{aligned} \frac{d\sigma_{\text{coll}}^{\text{LO}}}{dx_Q dx_J d^2 \vec{p}_Q d^2 \vec{p}_J} &= \sum_{i,j=q,\bar{q},g} \int_0^1 dx_i \int_0^1 dx_j \\ &\times f_i(x_a) f_j(x_b) \int_{x_Q}^1 \frac{dz}{z} D_i^Q \left(\frac{x_Q}{z} \right) \frac{d\hat{\sigma}_{i,j}(\hat{s})}{dx_Q dx_J d^2 \vec{p}_Q d^2 \vec{p}_J}. \end{aligned} \quad (4)$$

Here the i, j indices indicate the parton species (quarks $q = u, d, s, c, b$; antiquarks $\bar{q} = \bar{u}, \bar{d}, \bar{s}, \bar{c}, \bar{b}$; or gluon g), $f_{i,j}(x_{a,b}, \mu_F)$ are the PDFs, while $D_i^Q(x/z, \mu_F)$ denote

the quarkonium FFs; $x_{a,b}$ are the longitudinal momentum fractions of the partons initiating the hard subprocess and z the longitudinal fraction of the single parton that fragments into \mathcal{Q} . Finally, $d\hat{\sigma}_{i,j}(\hat{s})$ is the partonic cross section, with $\hat{s} \equiv x_a x_b s$ the squared center-of-mass energy of the partonic collision.

Contrariwise to the pure collinear treatment, we build the cross section in the hybrid factorization, where the high-energy dynamics is genuinely provided by the BFKL approach, and collinear ingredients are then embodied. We decompose the cross section as a Fourier sum of azimuthal-angle coefficients, \mathcal{C}_n , in the following way

$$\frac{(2\pi)^2 d\sigma}{dy_Q dy_J d\vec{p}_Q d\vec{p}_J d\phi_Q d\phi_J} = \left[\mathcal{C}_0 + 2 \sum_{n=1}^{\infty} \cos(n\varphi) \mathcal{C}_n \right], \quad (5)$$

where $\varphi_{Q,J}$ are azimuthal angles of the detected particles and $\varphi = \phi_Q - \phi_J - \pi$. The azimuthal coefficients $\mathcal{C}_n \equiv \mathcal{C}_n^{\text{NLA}}$ are computed in the BFKL framework and they contain the resummation of energy logarithms up to the NLA accuracy. In the $\overline{\text{MS}}$ renormalization scheme, the NLA expression for $\mathcal{C}_n^{\text{NLA}}$ reads (see, *e.g.*, Ref. [38])

$$\begin{aligned} \mathcal{C}_n^{\text{NLA}} &= \int_0^{2\pi} d\phi_Q \int_0^{2\pi} d\phi_J \cos(n\varphi) \\ &\times \frac{d\sigma_{\text{NLA}}}{dy_Q dy_J d|\vec{p}_Q| d|\vec{p}_J| d\phi_Q d\phi_J} = \int_{-\infty}^{+\infty} d\nu \frac{e^{\Delta Y \bar{\alpha}_s(\mu_R) \chi(n,\nu)}}{e^{-\Delta Y_s}} \\ &\times e^{\Delta Y \bar{\alpha}_s^2(\mu_R) \left[\bar{\chi}(n,\nu) + \frac{\beta_0}{8N_c} \chi(n,\nu) \left[\frac{10}{3} - \chi(n,\nu) + 4 \ln \left(\frac{\mu_R}{\sqrt{|\vec{p}_Q||\vec{p}_J|}} \right) \right] \right]} \\ &\times \alpha_s^2(\mu_R) \left[c_Q^{\text{NLO}}(n, \nu, |\vec{p}_Q|, x_1) [c_J^{\text{NLO}}(n, \nu, |\vec{p}_J|, x_2)]^* \right. \\ &\left. + \bar{\alpha}_s^2(\mu_R) \Delta Y \frac{\beta_0}{4N_c} \chi(n, \nu) f(\nu) \right], \end{aligned} \quad (6)$$

with $\bar{\alpha}_s(\mu_R) \equiv \alpha_s(\mu_R) N_c / \pi$, N_c the color number and $\beta_0 = 11N_c/3 - 2n_f/3$ the first coefficient of the QCD β -function. The Lipatov characteristic function is given by

$$\chi(n, \nu) = 2 \left\{ \psi(1) - \text{Re} \left[\psi \left(i\nu + \frac{1}{2} + \frac{n}{2} \right) \right] \right\} \quad (7)$$

where $\psi(z) = \Gamma'(z)/\Gamma(z)$ is the logarithmic derivative of the Gamma function. The $\bar{\chi}(n, \nu)$ function in Eq. (6)

contains NLO corrections to the BFKL kernel and was calculated in Ref. [108] (see also Ref. [109]). The two functions

$$\begin{aligned} c_{Q,J}^{\text{NLO}}(n, \nu, |\vec{p}|, x) &= c_{Q,J}(n, \nu, |\vec{p}|, x) \\ &+ \alpha_s(\mu_R) \hat{c}_{Q,J}(n, \nu, |\vec{p}|, x) \end{aligned} \quad (8)$$

are the impact factors for the production of a heavy-quarkonium state and for the emission of a light jet. Their LO parts read

$$\begin{aligned} c_Q(n, \nu, |\vec{p}|, x) &= 2 \sqrt{\frac{C_F}{C_A}} \frac{(|\vec{p}|^2)^{i\nu}}{|\vec{p}|} \int_x^1 \frac{d\zeta}{\zeta} \left(\frac{\zeta}{x} \right)^{2i\nu-1} \\ &\times \left[\frac{C_A}{C_F} f_g(\zeta) D_g^Q \left(\frac{x}{\zeta} \right) + \sum_{\alpha=q,\bar{q}} f_\alpha(\zeta) D_\alpha^Q \left(\frac{x}{\zeta} \right) \right] \end{aligned} \quad (9)$$

and

$$\begin{aligned} c_J(n, \nu, |\vec{p}|, x) &= 2 \sqrt{\frac{C_F}{C_A}} (|\vec{p}|^2)^{i\nu-1/2} \\ &\times \left(\frac{C_A}{C_F} f_g(x) + \sum_{\beta=q,\bar{q}} f_\beta(x) \right), \end{aligned} \quad (10)$$

respectively. The $f(\nu)$ function is defined in terms of the logarithmic derivative of LO impact factors

$$f(\nu) = \frac{i}{2} \frac{d}{d\nu} \ln \left(\frac{c_Q}{c_J^*} \right) + \ln(|\vec{p}_Q||\vec{p}_J|). \quad (11)$$

The remaining functions in Eq. (6) are the NLO impact-factor corrections, $\hat{c}_{Q,J}$. The NLO correction to the Q impact factor is calculated in the light-quark limit [110]. This option is fully consistent with our VFNS treatment, provided that the p_Q values at work are much larger than the heavy-quark mass.

3 Quarkonium fragmentation functions

NLO collinear FF sets for the *direct* J/ψ or Υ meson production are constructed by taking, as a starting point, a NLO calculation [105] for the heavy-quark FF portraying the transition $c \rightarrow J/\psi$ or the $b \rightarrow \Upsilon$ one, where c (b) indistinctly refer to the charm (bottom) quark and

its antiquark. It basically relies on the NRQCD factorization formalism (see, *e.g.*, Refs. [111–116]), in which the FF function of a parton i fragmenting into a heavy quarkonium \mathcal{Q} with longitudinal fraction z is written as

$$D_i^{\mathcal{Q}}(z, \mu_F) = \sum_{[n]} \mathcal{D}_i^{\mathcal{Q}}(z, \mu_F, [n]) \langle \mathcal{O}^{\mathcal{Q}}([n]) \rangle. \quad (12)$$

In Eq. (12), $\mathcal{D}_i(z, \mu_F, [n])$ is the short-distance perturbative coefficient, while $\langle \mathcal{O}^{\mathcal{Q}}([n]) \rangle$ is the NRQCD LDME. The summation is extended over all quarkonium quantum numbers $[n] \equiv {}^{2S+1}L_J^{(c)}$, in the spectroscopic notation, the (c) superscript identifying the color state, singlet (1) or octet (8).

We consider here only a spin-triplet (vector) and color-singlet quarkonium state, ${}^3S_1^{(1)}$. The form of the initial-scale FF portraying the constituent heavy-quark to quarkonium transition, $Q \rightarrow \mathcal{Q}$, reads [105]

$$\begin{aligned} D_Q^{\mathcal{Q}}(z, \mu_F \equiv \mu_0) &= D_Q^{\mathcal{Q},\text{LO}}(z) \\ &+ \frac{\alpha_s^3(3m_Q)}{m_Q^3} |\mathcal{R}_{\mathcal{Q}}(0)|^2 \Gamma_Q^{\mathcal{Q},\text{NLO}}(z), \end{aligned} \quad (13)$$

with $m_c = 1.5$ GeV or $m_b = 4.9$ GeV, and the radial wave-function at the origin of the quarkonium state set to [117]

$$|\mathcal{R}_{J/\psi}(0)|^2 = 0.810 \text{ GeV}^3$$

or to

$$|\mathcal{R}_Y(0)|^2 = 6.477 \text{ GeV}^3.$$

The LO initial-scale FF reads [118]

$$\begin{aligned} D_Q^{\mathcal{Q},\text{LO}}(z) &= \frac{\alpha_s^2(3m_Q)}{m_Q^3} \frac{8z(1-z)^2}{27\pi(2-z)^6} |\mathcal{R}_{\mathcal{Q}}(0)|^2 \\ &\times (5z^4 - 32z^3 + 72z^2 - 32z + 16), \end{aligned} \quad (14)$$

and the polynomial function $\Gamma_Q^{\mathcal{Q},\text{NLO}}(z)$ entering the expression for the NLO-FF correction is of the form

$$\Gamma_Q^{\mathcal{Q},\text{NLO}}(z) = \sum_{n=0}^{10} c_n z^n. \quad (15)$$

Coefficients of z -powers in Eqs. (15) can be found in Ref. [105]. They are obtained via a polynomial fit to the

numerically-calculated NLO FFs. Starting from $\mu_F \equiv \mu_0 = 3m_Q$, in Ref. [105] a DGLAP-evolved formula for the $D_Q^{\mathcal{Q}}(z, \mu_F)$ function was derived and then applied to phenomenological studies of J/ψ and Υ production via e^+e^- single inclusive annihilation (SIA). In all predictions we will use this FF, to which, from now, we refer as ZCW19.

4 Phenomenology

Numerical analysis was carried out by using JETHAD modular work package [101]. Sensitivity to scale variation of our predictions is evaluated allowing the ratio $C_\mu = \mu_{R,F}/\mu_N$ to vary from 1/2 to two. The error related to phase-space multi-dimensional integration is embodied and it is always kept below 1% by the JETHAD integrators. All calculations of our observables are done in the $\overline{\text{MS}}$ scheme. BLM scales are calculated in the MOM scheme.

4.1 ΔY -distribution

We start our phenomenological analysis by considering the φ -summed cross section differential in the $\Delta Y \equiv y_{\mathcal{Q}} - y_J$ interval or ΔY -distribution. It is obtained by integrating the \mathcal{C}_0 (see Eq. (6)) over transverse momenta and rapidities of the two emitted objects, and imposing a fixed value of ΔY . One has

$$\begin{aligned} \mathcal{C}_0 &= \int_{y_{\mathcal{Q}}^{\min}}^{y_{\mathcal{Q}}^{\max}} dy_{\mathcal{Q}} \int_{y_J^{\min}}^{y_J^{\max}} dy_J \int_{p_{\mathcal{Q}}^{\min}}^{p_{\mathcal{Q}}^{\max}} d|\vec{p}_{\mathcal{Q}}| \int_{p_J^{\min}}^{p_J^{\max}} d|\vec{p}_J| \\ &\times \delta(\Delta Y - (y_{\mathcal{Q}} - y_J)) \mathcal{C}_0(|\vec{p}_{\mathcal{Q}}|, |\vec{p}_J|, y_{\mathcal{Q}}, y_J). \end{aligned} \quad (16)$$

The light jet is tagged in kinematic configurations typical of current studies at the CMS detector [119], namely $35 \text{ GeV} < p_J < 60 \text{ GeV}$ and $|y_J| < 4.7$. The quarkonium transverse momentum is chosen to be in the range $20 \text{ GeV} < |\vec{p}_{\mathcal{Q}}| < 60 \text{ GeV}$, for consistency with the VFNS treatment. Concerning the rapidity range of the quarkonia, we allow the detection to be done only by the CMS barrel detector and not by endcaps, *i.e.* $|y_{\mathcal{Q}}| < 2.4$.

In Fig. 1 we compare the NLA ΔY -behavior of \mathcal{C}_0 with the corresponding prediction at LLA, in the J/ψ -plus-jet channel (left) and in the J/ψ -plus- J/ψ channel (right). We note that values of \mathcal{C}_0 are everywhere

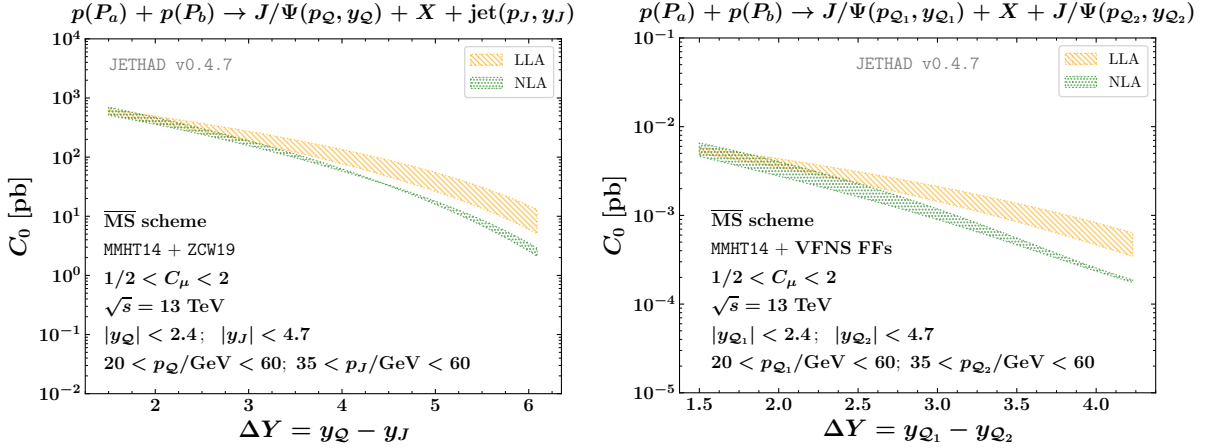


Fig. 1 ΔY -distribution in the $J/\psi + \text{jet}$ (left) and in the $J/\psi + J/\psi$ (right) channel, at $\sqrt{s} = 13$ TeV. Quarkonium fragmentation is described in terms of ZCW19 collinear FFs.

larger than 0.5 pb in the J/ψ -plus-jet channel (left). Although being substantially lower than the one for heavy-baryon and heavy-light meson emissions [88, 89], the statistics is promising. The downtrend with ΔY of our distributions both at LLA and NLA is a common feature of all the hadronic semi-hard reactions investigated so far. Although the high-energy resummation predicts a growth with energy of the partonic-subprocess cross section, its convolution with parent gluon PDFs leads, as a net effect, to a falloff with ΔY of both LLA and NLA predictions. We observe a partial stabilization of the high-energy series, with NLA bands almost overlapped to LLA ones at lower values of ΔY , and their mutual distance becoming wider in the large- ΔY range. In the left panel of Fig. 2 we corroborate our stability claims by carrying out a systematic study under variation of scale. We allow the ratio C_μ to vary between 1 and 30, noting that there are no very significant variations, especially at high ΔY .

4.2 φ -distribution

The second observable that we consider in our phenomenological analysis is the φ -distribution, or simply

azimuthal distribution, defined as

$$\begin{aligned} \frac{1}{\sigma} \frac{d\sigma}{d\varphi} &= \frac{1}{2\pi} \left\{ 1 + 2 \sum_{n=1}^{\infty} \cos(n\varphi) \langle \cos(n\varphi) \rangle \right\} \\ &= \frac{1}{2\pi} \left\{ 1 + 2 \sum_{n=1}^{\infty} \cos(n\varphi) R_{n0} \right\}, \end{aligned} \quad (17)$$

where $R_{n0} = C_n/C_0$ (with C_n being the azimuthal coefficient conformal spin n , integrated over the final-state phase space in the same way as in Eq. (16)). We checked the numerical stability of our calculation by progressively raising the effective upper limit of the n -sum in Eq. (17). An excellent numerical convergence was found at $n_{\max} = 20$. We adopt the same final-state kinematic cuts introduced in subsection 4.1.

In the right panel of Fig. 2 we present predictions for the azimuthal distribution as a function of φ and for three distinct values of the rapidity interval, $\Delta Y = 1, 3, 5$, in the $J/\psi + \text{jet}$ channel. Results were obtained by making use of the ZCW19 set.

The peculiar behavior of these observables corroborates the assumption that we are probing a regime where the BFKL treatment is valid. All distributions present a distinct peak at $\varphi = 0$, namely when the quarkonium and the jet are emitted in back-to-back configurations. When ΔY increases, the peak height decreases, while the distribution width broadens. This reflects the fact

that larger rapidity intervals bring to a more significant decorrelation of the quarkonium-jet system, so that the number of back-to-back events diminish.

5 Conclusion and outlook

The general outcomes of results presented in this work are:

- Inclusive forward J/ψ emissions, accompanied by a light-jet emissions lead to a favorable statistics for the ΔY -differential cross section. Effects of stabilization of the high-energy resummation under higher-order corrections and scale variation are considered.
- Studying the azimuthal distribution of quarkonium-plus-jet processes around natural values of μ_R and μ_F scales is feasible. This observable can be easily measured at the LHC, thus offering us the possibility of doing stringent tests of the high-energy resummation.

As anticipated, a more complete analysis including the production channel initiated by gluon (through the ZCW19⁺ FF set built in terms of both the constituent heavy-quark FF [105] and the gluon one [120]) and the study of emissions of the Υ , can be found in [92]. This work represents a further step in our ongoing program on heavy-flavored emissions and the natural continuation is the possible matching between our VFNS analysis and the approach developed in Ref. [83].

Remarkably, single-forward vector-quarkonium emissions offer us a peerless opportunity to access the proton structure at low x . In particular, they represent golden channels to study the *unintegrated gluon density* (UGD), whose low- x evolution is controlled by the BFKL equation. The information on the UGD gathered by quarkonium studies [121–123] will complement the one already known from deep-inelastic-scattering structure functions [124], light vector-meson helicity amplitudes and cross sections [125–137], and forward Drell–Yan di-lepton distributions [138–141]. Moreover, observables sensitive to quarkonium production are relevant to shed light on the intersection regime between the BFKL UGD and (un)polarized transverse-momentum-dependent gluon densities [142–149].

Acknowledgments

F.G.C. acknowledges support from the INFN/NINPHA project and thanks the Università degli Studi di Pavia for the warm hospitality. M.F. acknowledges support from the INFN/QFT@COLLIDERS project.

References

1. E. Chapon et al., Prog. Part. Nucl. Phys. **122**, 103906 (2022), [2012.14161](#).
2. L. A. Anchordoqui et al., Phys. Rept. **968**, 1 (2022), [2109.10905](#).
3. J. L. Feng et al. (2022), [2203.05090](#).
4. F. G. Celiberto, Phys. Rev. D **105**, 114008 (2022), [2204.06497](#).
5. M. Hentschinski et al., in *2022 Snowmass Summer Study* (2022), [2203.08129](#).
6. A. Accardi et al., Eur. Phys. J. A **52**, 268 (2016), [1212.1701](#).
7. R. Abdul Khalek et al. (2021), [2103.05419](#).
8. R. Abdul Khalek et al., in *2022 Snowmass Summer Study* (2022), [2203.13199](#).
9. D. Acosta, E. Barberis, N. Hurley, W. Li, O. M. Colin, D. Wood, and X. Zuo, in *2022 Snowmass Summer Study* (2022), [2203.06258](#).
10. I. Adachi et al. (ILC International Development Team and ILC Community) (2022), [2203.07622](#).
11. F. G. Celiberto, L. Jenkovszky, and V. Myronenko, EPJ Web Conf. **125**, 04012 (2016), [1608.04646](#).
12. F. G. Celiberto, R. Fiore, and L. Jenkovszky, AIP Conf. Proc. **1819**, 030005 (2017), [1612.00797](#).
13. O. Brunner et al. (2022), [2203.09186](#).
14. A. Arbuzov et al., Prog. Part. Nucl. Phys. **119**, 103858 (2021), [2011.15005](#).
15. V. M. Abazov et al. (SPD proto) (2021), [2102.00442](#).
16. G. Bernardi et al. (2022), [2203.06520](#).
17. S. Amoroso et al., in *2022 Snowmass Summer Study* (2022), [2203.13923](#).
18. F. G. Celiberto, M. Fucilla, D. Yu. Ivanov, M. M. A. Mohammed, and A. Papa, in *2022 Snowmass Summer Study* (2021).
19. S. Klein et al. (2020), [2009.03838](#).

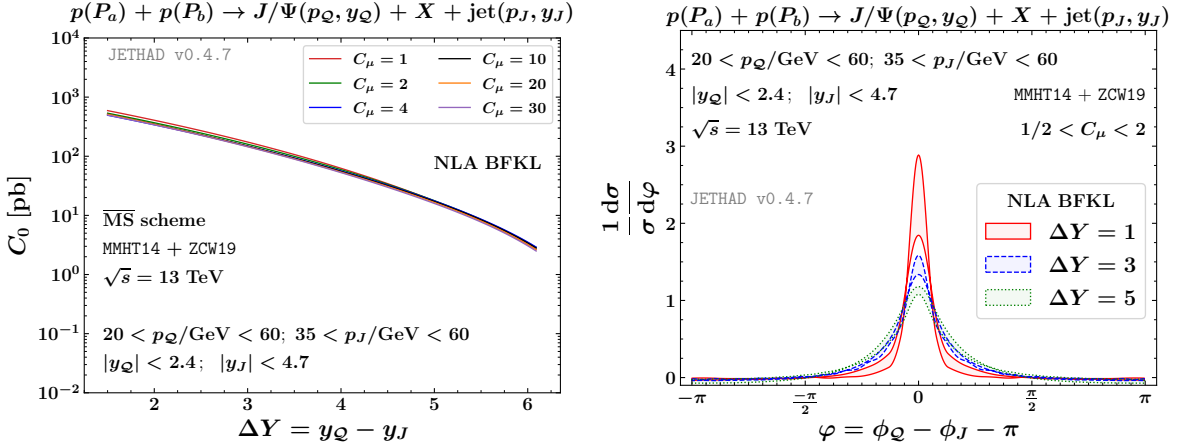


Fig. 2 In the left panel, ΔY -distribution in the $J/\psi + \text{jet}$ for $C_\mu = 1, 2, 4, 10, 20, 30$ at 13 TeV. In the right panel, NLA predictions for the φ -distribution in the $J/\psi + \text{jet}$ channel, at $\sqrt{s} = 13$ TeV, and for three distinct values of ΔY . Quarkonium fragmentation is described in terms of ZCW19 collinear FFs.

20. A. Canepa and M. D'Onofrio (2022).
21. J. de Blas et al. (Muon Collider) (2022), [2203.07261](#).
22. C. Aimè et al. (2022), [2203.07256](#).
23. L. V. Gribov, E. M. Levin, and M. G. Ryskin, Phys. Rept. **100**, 1 (1983).
24. F. G. Celiberto, Ph.D. thesis, Università della Calabria and INFN-Cosenza (2017), [1707.04315](#).
25. V. S. Fadin, E. Kuraev, and L. Lipatov, Phys. Lett. B **60**, 50 (1975).
26. E. A. Kuraev, L. N. Lipatov, and V. S. Fadin, Sov. Phys. JETP **44**, 443 (1976).
27. E. Kuraev, L. Lipatov, and V. S. Fadin, Sov. Phys. JETP **45**, 199 (1977).
28. I. Balitsky and L. Lipatov, Sov. J. Nucl. Phys. **28**, 822 (1978).
29. V. S. Fadin and L. N. Lipatov, Phys. Lett. B **429**, 127 (1998), [hep-ph/9802290](#).
30. M. Ciafaloni and G. Camici, Phys. Lett. B **430**, 349 (1998), [hep-ph/9803389](#).
31. V. S. Fadin, R. Fiore, and A. Papa, Phys. Rev. D **60**, 074025 (1999), [hep-ph/9812456](#).
32. V. S. Fadin and D. A. Gorbachev, JETP Lett. **71**, 222 (2000).
33. V. S. Fadin and D. A. Gorbachev, Phys. Atom. Nucl. **63**, 2157 (2000).
34. V. S. Fadin and R. Fiore, Phys. Lett. B **610**, 61 (2005), [Erratum: Phys.Lett.B 621, 320 (2005)], [hep-ph/0412386](#).
35. V. S. Fadin and R. Fiore, Phys. Rev. D **72**, 014018 (2005), [hep-ph/0502045](#).
36. A. H. Mueller and H. Navelet, Nucl. Phys. B **282**, 727 (1987).
37. D. Colferai, F. Schwennsen, L. Szymanowski, and S. Wallon, JHEP **12**, 026 (2010), [1002.1365](#).
38. F. Caporale, D. Ivanov, B. Murdaca, and A. Papa, Nucl. Phys. B **877**, 73 (2013), [1211.7225](#).
39. B. Ducloué, L. Szymanowski, and S. Wallon, JHEP **05**, 096 (2013), [1302.7012](#).
40. B. Ducloué, L. Szymanowski, and S. Wallon, Phys. Rev. Lett. **112**, 082003 (2014), [1309.3229](#).
41. F. Caporale, B. Murdaca, A. Sabio Vera, and C. Salas, Nucl. Phys. B **875**, 134 (2013), [1305.4620](#).
42. F. Caporale, D. Yu. Ivanov, B. Murdaca, and A. Papa, Eur. Phys. J. C **74**, 3084 (2014), [Erratum: Eur.Phys.J.C 75, 535 (2015)], [1407.8431](#).
43. D. Colferai and A. Niccoli, JHEP **04**, 071 (2015), [1501.07442](#).
44. F. Caporale, D. Yu. Ivanov, B. Murdaca, and A. Papa, Phys. Rev. D **91**, 114009 (2015), [1504.06471](#).

-
45. B. Ducloué, L. Szymanowski, and S. Wallon, Phys. Rev. D **92**, 076002 (2015), [1507.04735](#).
46. F. G. Celiberto, D. Yu. Ivanov, B. Murdaca, and A. Papa, Eur. Phys. J. C **75**, 292 (2015), [1504.08233](#).
47. F. G. Celiberto, D. Yu. Ivanov, B. Murdaca, and A. Papa, Acta Phys. Polon. Supp. **8**, 935 (2015), [1510.01626](#).
48. F. G. Celiberto, D. Yu. Ivanov, B. Murdaca, and A. Papa, Eur. Phys. J. C **76**, 224 (2016), [1601.07847](#).
49. F. G. Celiberto, D. Yu. Ivanov, B. Murdaca, and A. Papa, PoS **DIS2016**, 176 (2016), [1606.08892](#).
50. F. Caporale, F. G. Celiberto, G. Chachamis, D. Gordo Gómez, and A. Sabio Vera, Nucl. Phys. B **935**, 412 (2018), [1806.06309](#).
51. N. B. de León, G. Chachamis, and A. Sabio Vera, Eur. Phys. J. C **81**, 1019 (2021), [2106.11255](#).
52. F. G. Celiberto and A. Papa (2022), [2207.05015](#).
53. F. G. Celiberto, D. Yu. Ivanov, B. Murdaca, and A. Papa, Phys. Rev. D **94**, 034013 (2016), [1604.08013](#).
54. F. G. Celiberto, D. Yu. Ivanov, B. Murdaca, and A. Papa, AIP Conf. Proc. **1819**, 060005 (2017), [1611.04811](#).
55. F. G. Celiberto, D. Yu. Ivanov, B. Murdaca, and A. Papa, Eur. Phys. J. C **77**, 382 (2017), [1701.05077](#).
56. F. G. Celiberto, D. Yu. Ivanov, B. Murdaca, and A. Papa, in *25th Low-x Meeting* (2017), [1709.01128](#).
57. F. G. Celiberto, D. Yu. Ivanov, B. Murdaca, and A. Papa, in *17th conference on Elastic and Diffractive Scattering* (2017), [1709.04758](#).
58. F. Caporale, G. Chachamis, B. Murdaca, and A. Sabio Vera, Phys. Rev. Lett. **116**, 012001 (2016), [1508.07711](#).
59. F. Caporale, F. G. Celiberto, G. Chachamis, and A. Sabio Vera, Eur. Phys. J. C **76**, 165 (2016), [1512.03364](#).
60. F. Caporale, F. G. Celiberto, G. Chachamis, D. Gordo Gómez, and A. Sabio Vera, Nucl. Phys. B **910**, 374 (2016), [1603.07785](#).
61. F. Caporale, F. G. Celiberto, G. Chachamis, and A. Sabio Vera, PoS **DIS2016**, 177 (2016), [1610.01880](#).
62. F. Caporale, F. G. Celiberto, G. Chachamis, D. Gordo Gómez, and A. Sabio Vera, Eur. Phys. J. C **77**, 5 (2017), [1606.00574](#).
63. F. G. Celiberto, Frascati Phys. Ser. **63**, 43 (2016), [1606.07327](#).
64. F. Caporale, F. G. Celiberto, G. Chachamis, D. Gordo Gómez, and A. Sabio Vera, AIP Conf. Proc. **1819**, 060009 (2017), [1611.04813](#).
65. F. Caporale, F. G. Celiberto, G. Chachamis, D. Gordo Gomez, B. Murdaca, and A. Sabio Vera, in *24th Low-x Meeting* (2017), vol. 5, p. 47, [1610.04765](#).
66. G. Chachamis, F. Caporale, F. Celiberto, D. Gomez Gordo, and A. Sabio Vera, PoS **DIS2016**, 178 (2016).
67. G. Chachamis, F. Caporale, F. G. Celiberto, D. G. Gomez, and A. Sabio Vera (2016), [1610.01342](#).
68. F. Caporale, F. G. Celiberto, G. Chachamis, D. Gordo Gómez, and A. Sabio Vera, EPJ Web Conf. **164**, 07027 (2017), [1612.02771](#).
69. F. Caporale, F. G. Celiberto, G. Chachamis, D. Gordo Gómez, and A. Sabio Vera, Phys. Rev. D **95**, 074007 (2017), [1612.05428](#).
70. G. Chachamis, F. Caporale, F. G. Celiberto, D. Gordo Gomez, and A. Sabio Vera, PoS **DIS2017**, 067 (2018), [1709.02649](#).
71. F. Caporale, F. G. Celiberto, D. Gordo Gomez, A. Sabio Vera, and G. Chachamis, in *25th Low-x Meeting* (2017), [1801.00014](#).
72. A. D. Bolognino, F. G. Celiberto, D. Yu. Ivanov, M. M. Mohammed, and A. Papa, Eur. Phys. J. C **78**, 772 (2018), [1808.05483](#).
73. A. D. Bolognino, F. G. Celiberto, D. Yu. Ivanov, M. M. A. Mohammed, and A. Papa, PoS **DIS2019**, 049 (2019), [1906.11800](#).
74. A. D. Bolognino, F. G. Celiberto, D. Yu. Ivanov, M. M. Mohammed, and A. Papa, Acta Phys. Polon. Supp. **12**, 773 (2019), [1902.04511](#).
75. F. G. Celiberto, D. Yu. Ivanov, and A. Papa, Phys. Rev. D **102**, 094019 (2020), [2008.10513](#).

76. F. G. Celiberto, D. Yu. Ivanov, M. M. A. Mohammed, and A. Papa, Eur. Phys. J. C **81**, 293 (2021), [2008.00501](#).
77. F. G. Celiberto, D. Y. Ivanov, M. M. A. Mohammed, and A. Papa, SciPost Phys. Proc. **8**, 039 (2022), [2107.13037](#).
78. F. G. Celiberto, M. Fucilla, A. Papa, D. Yu. Ivanov, and M. M. A. Mohammed, PoS **EPS-HEP2021**, 589 (2022), [2110.09358](#).
79. F. G. Celiberto, M. Fucilla, D. Yu. Ivanov, M. M. A. Mohammed, and A. Papa, PoS **PANIC2021**, 352 (2022), [2111.13090](#).
80. F. G. Celiberto, M. Fucilla, D. Yu. Ivanov, M. M. A. Mohammed, and A. Papa (2021), [2110.12649](#).
81. F. G. Celiberto, M. Fucilla, D. Y. Ivanov, M. M. A. Mohammed, and A. Papa, JHEP **08**, 092 (2022), [2205.02681](#).
82. K. Golec-Biernat, L. Motyka, and T. Stebel, JHEP **12**, 091 (2018), [1811.04361](#).
83. R. Boussarie, B. Ducloué, L. Szymanowski, and S. Wallon, Phys. Rev. D **97**, 014008 (2018), [1709.01380](#).
84. F. G. Celiberto, D. Yu. Ivanov, B. Murdaca, and A. Papa, Phys. Lett. B **777**, 141 (2018), [1709.10032](#).
85. A. D. Bolognino, F. G. Celiberto, M. Fucilla, D. Yu. Ivanov, B. Murdaca, and A. Papa, PoS **DIS2019**, 067 (2019), [1906.05940](#).
86. A. D. Bolognino, F. G. Celiberto, M. Fucilla, D. Yu. Ivanov, and A. Papa, Eur. Phys. J. C **79**, 939 (2019), [1909.03068](#).
87. A. D. Bolognino, F. G. Celiberto, M. Fucilla, D. Yu. Ivanov, B. Murdaca, and A. Papa, PoS **DIS2019**, 067 (2019), [1906.05940](#).
88. F. G. Celiberto, M. Fucilla, D. Yu. Ivanov, and A. Papa, Eur. Phys. J. C **81**, 780 (2021), [2105.06432](#).
89. F. G. Celiberto, M. Fucilla, D. Yu. Ivanov, M. M. A. Mohammed, and A. Papa, Phys. Rev. D **104**, 114007 (2021), [2109.11875](#).
90. A. D. Bolognino, F. G. Celiberto, M. Fucilla, D. Yu. Ivanov, and A. Papa, PoS **EPS-HEP2021**, 389 (2022).
91. A. D. Bolognino, F. G. Celiberto, M. Fucilla, D. Yu. Ivanov, and A. Papa, PoS **EPS-HEP2021**, 389 (2022), [2110.12772](#).
92. F. G. Celiberto and M. Fucilla, under revision in Eur. Phys. J. C (2022), [2202.12227](#).
93. F. G. Celiberto (2022), [2206.09413](#).
94. F. G. Celiberto, M. Fucilla, M. M. A. Mohammed, and A. Papa, Phys. Rev. D **105**, 114056 (2022), [2205.13429](#).
95. A. D. Bolognino, F. G. Celiberto, M. Fucilla, D. Yu. Ivanov, and A. Papa, Phys. Rev. D **103**, 094004 (2021), [2103.07396](#).
96. A. D. Bolognino, F. G. Celiberto, M. Fucilla, D. Yu. Ivanov, and A. Papa, SciPost Phys. Proc. **8**, 068 (2022), [2103.07396](#).
97. S. J. Brodsky, F. Hautmann, and D. E. Soper, Phys. Rev. Lett. **78**, 803 (1997), [Erratum: Phys. Rev. Lett. 79, 3544 (1997)], [hep-ph/9610260](#).
98. S. J. Brodsky, F. Hautmann, and D. E. Soper, Phys. Rev. D **56**, 6957 (1997), [hep-ph/9706427](#).
99. S. J. Brodsky, V. S. Fadin, V. T. Kim, L. N. Lipatov, and G. B. Pivovarov, JETP Lett. **70**, 155 (1999), [hep-ph/9901229](#).
100. S. J. Brodsky, V. S. Fadin, V. T. Kim, L. N. Lipatov, and G. B. Pivovarov, JETP Lett. **76**, 249 (2002), [hep-ph/0207297](#).
101. F. G. Celiberto, Eur. Phys. J. C **81**, 691 (2021), [2008.07378](#).
102. M. Hentschinski, K. Kutak, and A. van Hameren, Eur. Phys. J. C **81**, 112 (2021), [Erratum: Eur. Phys. J. C 81, 262 (2021)], [2011.03193](#).
103. B. Mele and P. Nason, Nucl. Phys. B **361**, 626 (1991), [Erratum: Nucl. Phys. B 921, 841–842 (2017)].
104. M. Cacciari and M. Greco, Nucl. Phys. B **421**, 530 (1994), [hep-ph/9311260](#).
105. X.-C. Zheng, C.-H. Chang, and X.-G. Wu, Phys. Rev. D **100**, 014005 (2019), [1905.09171](#).
106. R. Boussarie, B. Ducloué, L. Szymanowski, and S. Wallon, in *International Conference on the Structure and Interactions of the Photon and 21st International Workshop on Photon-Photon Collisions and International Workshop on High Energy Photon Linear Colliders* (2015), [1511.02181](#).

107. R. Boussarie, B. Ducloue, L. Szymanowski, and S. Wallon, PoS **DIS2016**, 204 (2016).
108. A. V. Kotikov and L. N. Lipatov, Nucl. Phys. B **582**, 19 (2000), [hep-ph/0004008](#).
109. A. V. Kotikov and L. N. Lipatov, Nucl. Phys. B **661**, 19 (2003), [Erratum: Nucl.Phys.B 685, 405–407 (2004)], [hep-ph/0208220](#).
110. D. Yu. Ivanov and A. Papa, JHEP **07**, 045 (2012), [1205.6068](#).
111. B. A. Thacker and G. P. Lepage, Phys. Rev. D **43**, 196 (1991).
112. G. T. Bodwin, E. Braaten, and G. P. Lepage, Phys. Rev. D **51**, 1125 (1995), [Erratum: Phys.Rev.D 55, 5853 (1997)], [hep-ph/9407339](#).
113. N. Brambilla et al. (Quarkonium Working Group) (2004), [hep-ph/0412158](#).
114. N. Brambilla et al., Eur. Phys. J. C **71**, 1534 (2011), [1010.5827](#).
115. A. Pineda, Prog. Part. Nucl. Phys. **67**, 735 (2012), [1111.0165](#).
116. N. Brambilla, H. S. Chung, and A. Vairo, Phys. Rev. Lett. **126**, 082003 (2021), [2007.07613](#).
117. E. J. Eichten and C. Quigg, Phys. Rev. D **49**, 5845 (1994), [hep-ph/9402210](#).
118. E. Braaten, K.-m. Cheung, and T. C. Yuan, Phys. Rev. D **48**, 4230 (1993), [hep-ph/9302307](#).
119. V. Khachatryan et al. (CMS), JHEP **08**, 139 (2016), [1601.06713](#).
120. E. Braaten and T. C. Yuan, Phys. Rev. Lett. **71**, 1673 (1993), [hep-ph/9303205](#).
121. I. Bautista, A. Fernandez Tellez, and M. Hentschinski, Phys. Rev. D **94**, 054002 (2016), [1607.05203](#).
122. A. Arroyo Garcia, M. Hentschinski, and K. Kutak, Phys. Lett. B **795**, 569 (2019), [1904.04394](#).
123. M. Hentschinski and E. Padrón Molina, Phys. Rev. D **103**, 074008 (2021), [2011.02640](#).
124. M. Hentschinski, A. Sabio Vera, and C. Salas, Phys. Rev. Lett. **110**, 041601 (2013), [1209.1353](#).
125. I. Anikin, D. Yu. Ivanov, B. Pire, L. Szymanowski, and S. Wallon, Nucl. Phys. B **828**, 1 (2010), [0909.4090](#).
126. I. Anikin, A. Besse, D. Yu. Ivanov, B. Pire, L. Szymanowski, and S. Wallon, Phys. Rev. D **84**, 054004 (2011), [1105.1761](#).
127. A. Besse, L. Szymanowski, and S. Wallon, JHEP **11**, 062 (2013), [1302.1766](#).
128. A. D. Bolognino, F. G. Celiberto, D. Yu. Ivanov, and A. Papa, Eur. Phys. J. **C78**, 1023 (2018), [1808.02395](#).
129. A. D. Bolognino, F. G. Celiberto, D. Yu. Ivanov, and A. Papa, Frascati Phys. Ser. **67**, 76 (2018), [1808.02958](#).
130. A. D. Bolognino, F. G. Celiberto, D. Yu. Ivanov, and A. Papa, Acta Phys. Polon. Supp. **12**, 891 (2019), [1902.04520](#).
131. A. D. Bolognino, A. Szczurek, and W. Schaefer, Phys. Rev. D **101**, 054041 (2020), [1912.06507](#).
132. F. G. Celiberto, Nuovo Cim. **C42**, 220 (2019), [1912.11313](#).
133. A. D. Bolognino, F. G. Celiberto, D. Yu. Ivanov, A. Papa, W. Schäfer, and A. Szczurek, Eur. Phys. J. C **81**, 846 (2021), [2107.13415](#).
134. A. D. Bolognino, F. G. Celiberto, D. Y. Ivanov, and A. Papa, SciPost Phys. Proc. **8**, 089 (2022), [2107.12725](#).
135. A. D. Bolognino, F. G. Celiberto, M. Fucilla, D. Yu. Ivanov, A. Papa, W. Schäfer, and A. Szczurek, in *19th International Conference on Hadron Spectroscopy and Structure* (2022), [2202.02513](#).
136. F. G. Celiberto (2022), [2202.04207](#).
137. A. D. Bolognino, F. G. Celiberto, D. Yu. Ivanov, A. Papa, W. Schäfer, and A. Szczurek, Zenodo, in press (2022), [2207.05726](#).
138. L. Motyka, M. Sadzikowski, and T. Stebel, JHEP **05**, 087 (2015), [1412.4675](#).
139. D. Brzemiński, L. Motyka, M. Sadzikowski, and T. Stebel, JHEP **01**, 005 (2017), [1611.04449](#).
140. L. Motyka, M. Sadzikowski, and T. Stebel, Phys. Rev. **D95**, 114025 (2017), [1609.04300](#).
141. F. G. Celiberto, D. Gordo Gómez, and A. Sabio Vera, Phys. Lett. **B786**, 201 (2018), [1808.09511](#).
142. A. Bacchetta, F. G. Celiberto, M. Radici, and P. Taels, Eur. Phys. J. C **80**, 733 (2020), [2005.02288](#).

-
- 143. F. G. Celiberto, Nuovo Cim. **C44**, 36 (2021), [2101.04630](#).
 - 144. A. Bacchetta, F. G. Celiberto, M. Radici, and P. Taels, SciPost Phys. Proc. **8**, 040 (2022), [2107.13446](#).
 - 145. A. Bacchetta, F. G. Celiberto, and M. Radici, PoS **EPS-HEP2021**, 376 (2022), [2111.01686](#).
 - 146. A. Bacchetta, F. G. Celiberto, and M. Radici, PoS **PANIC2021**, 378 (2022), [2111.03567](#).
 - 147. A. Bacchetta, F. G. Celiberto, and M. Radici (2022), [2201.10508](#).
 - 148. A. Bacchetta, F. G. Celiberto, and M. Radici (2022), [2206.07815](#).
 - 149. A. Bacchetta, F. G. Celiberto, M. Radici, and A. Signori (2022), [2208.06252](#).